UDC 624.048-033.26:621.651

Mykola Demchuk*, Master of Science,
Nadia Saiyouri,** Doctor of Ecole Centrale de Paris

*National University of Water Management and Natural Resources Use, Rivne,
**Research Institute of Civil and Mechanical Engineering (GeM),
Nantes, France

A REALIZATION OF THE UNCERTAINTY UNIFORMITY PRINCIPLE IN A GROUTING MODEL

A method of a realization of the uncertainty uniformity principle in grouting model calculations is described.

Key words: *method error, numerical solution analysis, uncertainty uniformity principle, high gradient region.*

Introduction. Before creations of foundations on weak soil plots, to make better elastic properties of soil tracts the grouting operations are performed. In this technique a cement grout is injected under high pressure (10—30 bars) into a dry porous medium or water saturated one. The aim is reached after the grout hardening. The infiltrate is composed of particles that can be responsible for the phenomenon called the deep bed filtration or the depth filtration. Depending on particle and pore throat sizes two limiting cases are distinguished in the description of this phenomenon. In the first case, large particles are trapped by small pore throats. Whereas in the second case, small particles deposit over large pore bodies and large pore throats that result in a gradual reduction of pore throat sizes [19, p. 1637].

Grouting is rather costly and time consuming. Its regime is determined by the concentration distribution evolution [12, p. 1195]. Therefore, a calculation of this evolution using mathematical modeling is important. A grouting model is only a simplified version of a real system containing a porous medium and an infiltrate. It is constructed to simulate the excitation-response relations of the modeled system [11, p. 11]. In article [3, p. 61—63] it was argued that under condition

$$\sqrt{V \cdot t} >> \sqrt{8 \cdot a_L} \qquad (1)$$

where V is the fluid particle velocity, a_L is the coefficient of the longitudinal dispersion of the cement concentration in the fluid phase during an injection of the grout in the water saturated porous medium, and t is the injection duration, the peculiarities of a solute propagation in a porous medium can be neglected, and grouting can be modeled by a problem with a free moving boundary (1) is usually satisfied in fieldworks [3, p. 72; 4, p. 123]. Therefore, if a grouting model does not belong to the class of

problems with free moving boundaries, then it can be referred to the class of problems about pollution propagations. Articles [5, p. 46; 12, p. 1215—1216; 15, p. 5—6; 16, p. 230—233] deal with modeling of the standard laboratory test described in the next section. In several papers [1, p. 675; 2, p. 269; 3, p. 63; 13, p. 670—671; 14, p. 1042—1043; 18, p. 166; 20, p. 211—212] a cement grout propagation in a porous medium is examined in configurations more realistic during in situ grouting. In part of them [14, p. 1048; 18, p. 166] it is indicated that the deep bed filtration is not a dominant phenomenon.

Existing models of a cement grout propagation in a porous medium use different sets of simplifying assumptions. In models [5, p. 48—50; 14, p. 1040—1041; 15, p. 2—3; 16, p. 228—230; 18, p. 165—168; 20, p. 212—214] the ground skeleton is regarded as absolutely rigid, while in models [1, p. 675—685; 2, p. 269—271; 3, p. 63—65; 12, p. 1211—1215; 13, p. 669—670] it is assumed to be deformable. In models [1, p. 675—685; 2, p. 269—271; 3, p. 63—65; 20, p. 212—214] peculiarities of a solute propagation in a porous medium are neglected, in model [18, p. 165—168] the hydromechanical dispersion and diffusion are neglected, and in models [15, p. 2—3; 5, p. 48—50] the deep bed filtration is not taken into account. In models [14, p. 1040—1041; 16, p. 228—230] the first limiting case is assumed in the depth filtration description, while in models [12, p. 121—1215; 13, p. 669—670; 18, p. 165—168] the second one is assumed. A comparison of model calculations with laboratory measurements and calculation consistency checks justify the set of assumptions used in a model formulation. Amounts of information they provide depend upon values of uncertainties in compared quantities [5, p. 46—47]. There are three types of numerical calculation errors: the error due to uncertainties in input data, the round off error, and the error of a calculation method [8, p. 11]. If input data are fixed, then the error of the first type is zero. If the finite difference scheme according to which the calculations are performed is conditionally stable, then the round off error is negligible. This property of the scheme is usually verified during a numerical solution analysis. Models [1, p. 675—685; 2, p. 269—271; 3, p. 63—65], and [20, p. 212—214] belong to the class of problems with free moving boundaries. Condition (1) implies high injection pressure values that are difficult to achieve in laboratory conditions. Therefore, calculations according to models of this type have not been compared with laboratory measurements yet. In each case considered in papers [2, p. 282—286; 3, p. 69—74], and [20, p. 218—221] the error of a numerical method of a calculation of the final injection front position was estimated using the assumption that a contribution of the uncertainty in this position due to the uncertainty in the

choice of a method of a free surface interpolation on each time layer to this error is negligible. In paper [4, p. 128—129] it is shown that results of calculations presented in [2, p. 282—286; 3, p. 69—74], and [20, p. 218—221] are consistent. Since these calculations were performed on scanty grids, this consistency check provides a small amount of information. In article [1, p. 675—685] the model solutions were found analytically. Since in the models belonging to the class of problems about pollution propagations [5, p. 48—50; 12, p. 1219—1222; 13, p. 672; 14, p. 1045—1046; 15, p. 6; 16, p. 238; 18, p. 169—171] the sought functions contain high gradient regions, according to the uncertainty uniformity principle [10, p. 35] to estimate the approximation errors properly in these models calculations on time layers should be performed on non-uniform grids with smaller space increments inside these regions and larger ones outside them. Positions of these high gradient regions are changing with time and not known in advance. Therefore, in these models calculation errors are not estimated. Instead, in papers [13, p. 675—676; 14, p. 1042], to prove that the chosen numerical methods are precise enough, the numerical solutions of benchmark problems obtained by these methods were compared with their precise analytical solutions. In paper [18, p. 168] in the limiting case of a small variation of porosity due to the depth filtration the analytical solution of the model was obtained. To justify the numerical procedure used in [18, p. 169—171] this analytical solution was compared with numerical solutions of the model [18, p. 166—168] valid for significant as well as small variations of porosity due to the deep bed filtration. The numerical methods used in papers [12, p. 1224; 16, p. 235] were validated in earlier articles. In article [15, p. 5], to circumvent numerical oscillations appearing near relatively sharp concentration fronts, the space and time increments were chosen to satisfy Courant and Peclet number restrictions. Calculations according to model [5, p. 48—50] have not been presented yet.

The aim of this work is to develop a method of a proper treatment of high gradient regions in sought functions during numerical calculations according to model [5, p. 48—50].

Uniaxial injection test. The injection tests are performed in vertical columns of height 0,75 m and 0,08 m in diameter filled with Loire sand (0,70 m). Loire sand characteristics are available in [17, p. 1—7]. The sand is put in place in the column by layers and a compaction method is used to get a fixed density. The injection is performed at a constant pumping rate $\left(q_{imp} = 1,5E-6\ m^3/s\right)$ after the sand has been saturated with water. The column is open at the top. The material properties are given in Table 1.

Three pressure transducers are positioned along the column and one at the bottom of the column (injection point). They are spaced out 0,2 m apart. The whole concentration field is not experimentally available, and only the grout front position can be obtained. It is detected by the acoustic emission (AE) using transducers coupled with three wave guides which cross the sand column. They are horizontally placed at the same height as the pressure transducers. An increase of the acoustic activity is observed when the grout reaches the wave guide. Consequently, the grout front position is able to be detected at different times and locations in the sand column. The technique of AE is validated by performing injection tests in transparent columns. In this case, the grout propagation is visually followed, to ensure that the AE detection really occurred when the grout arrived at the wave guide. During injection tests the volume and the weight of injected grout, the pumping pressure, and the pumping rate are also recorded.

Table 1

Material properties

Porosity	0,335
Grout density	$1370\ \ kg/m^3$
Grout viscosity	$2,9\times10^{-3}\ \ Pa\cdot s$
Intrinsic permeability	$1,17\times10^{-11}\ \ m^2$
Diffusion coefficient	$1,0\times10^{-10}\ \ m^2/s$
Longitudinal dispersion coefficient	$2,0\times10^{-2}\ \ m$
Compressibility coefficient	$3,0\times10^{-8}\ \ Pa^{-1}$
Water viscosity	$1,1\times10^{-3}\ \ Pa\cdot s$

Figures (1a), (1b), and (1c) show the acoustic activity recorded by AE versus time for three transducers c1, c2, and c3 associated with the wave guides. Transducers c1, c2, and c3 detect the grout front at moments of time $t_1 = 100\ \boldsymbol{s}$, $t_2 = 250\ \boldsymbol{s}$, and $t_3 = 400\ \boldsymbol{s}$ respectively. Since they are spaced out 0,2 m apart, the fluid particle velocity can be estimated as

$$V = 0,2\ m/150\ s = 1,33\times10^{-3}\ \ m/s\,. \qquad (2)$$

Using data from Table 1 one can estimate $\sqrt{8a_L/V} \approx 11\sqrt{s}$. Comparing this value with $\sqrt{t_1}$, $\sqrt{t_2}$, and $\sqrt{t_3}$ we can conclude that condition (1) is not satisfied. Figure (1d) shows the evolution of the experimental injection pressure with time. It exhibits oscillations due to vibrations of the pump during the injection.

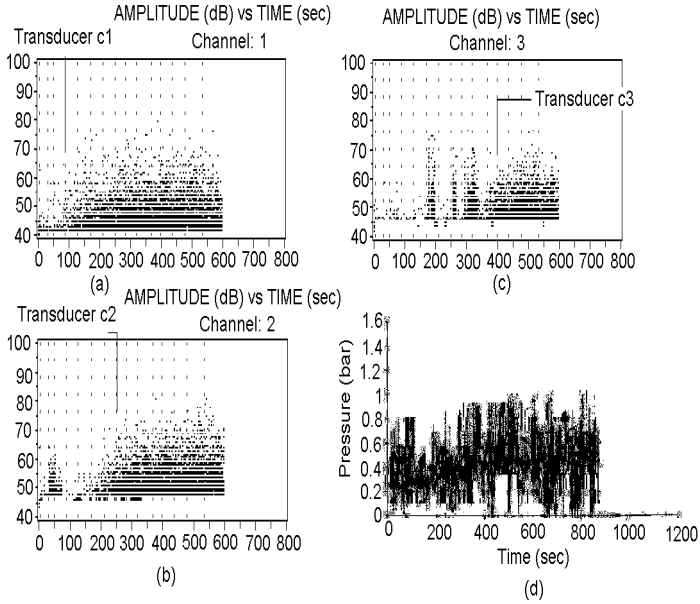

Fig. 1. *(a), (b), (c) Grout propagation followed by transducers c1, c2, c3. (d) Evolution of the experimental injection pressure with time*

A grouting model belonging to the class of problems about pollution propagations. We assume that the coordinate origin is chosen at the injection point and that the coordinate axis is directed upward. In this work we use the following notations. ε is a small positive parameter, α_0 and α_1 are large positive parameters. They are introduced in the model to conform initial conditions with boundary conditions, and their values will be obtained later in the result of the analysis of the numerical solutions. $I = (-\varepsilon,\ L)$ is an interval (a set of points $(x):\ x \in (-\varepsilon,\ L)$). $I_T = I \times (0,\ T)$ is a rectangle (a set of points $(x,\ t):\ (x) \in I,\ t \in (0,\ T)$), $A_{T,1}$ is the bottom side of I_T (a set of points $(-\varepsilon,\ t):\ t \in [0,\ T]$), $A_{T,2}$ is the top side of I_T (a set of points $(L,\ t):\ t \in [0,\ T]$), $p(x,t)$ and $c(x,t)$ denote the pore fluid pressure and the grout concentration respectively. K is the permeability of the medium, m is the medium porosity, ρ is the fluid phase density, g is the acceleration of free fall, μ_1 and c_{imp} are the grout viscosity and the grout concentration inside the injector respectively, μ_2 is the water viscosity. a_L is the longitudinal dispersion coefficient, D^* is the diffusion coefficient,

$\mu = (\mu_1 - \mu_2)c/c_{imp} + \mu_2$, $D_h = a_L V + D^*$, $V = -K(\partial p/\partial x + \rho g)/\mu/m$.

$f_\theta(\alpha \cdot x)$ is the function that tends to the function

$$\theta(x) = \begin{cases} 0, & if\ x < 0, \\ 1/2, & if\ x = 0, \\ 1, & if\ x > 0, \end{cases} \tag{3}$$

with $\alpha \to +\infty$ [6, p. 677]. S is the area of the interface between the injector and the porous medium, L is the tube length,

$$\mu_{L,0} = (\mu_1 - \mu_2)\left(1 - f_\theta(\alpha_0 L)\right) + \mu_2,$$

$$\mu_{0,0} = (\mu_1 - \mu_2)\left(1 - f_\theta(-\alpha_0 \varepsilon)\right) + \mu_2,$$

$$V_{L,0} = \mu_1 V_0 \left(1 - f_\theta(\alpha_1 x) - x\, df(\alpha_1 x)/dx\right)_{x=L} / \mu_{L,0},\ V_0 = q_{imp}/S/m.$$

In recent paper [5, p. 48—50] the mathematical model of the laboratory experiment described in the previous section with boundary conditions conforming to initial ones has been formulated. In it the ground skeleton is regarded as absolutely rigid and the deep bed filtration is not taken into account. This model is the following system of two partial differential equations valid for such values x and t that $(x,\ t) \in I_T$

$$m\,\partial c/\partial t = -mV \cdot \partial c/\partial x + \partial\left(mD_h \cdot \partial c/\partial x\right)/\partial x, \tag{4}$$

$$m\beta_p\left(\partial p/\partial t + V\,\partial p/\partial x\right) - \partial\left(K\left(\partial p/\partial x + \rho g\right)/\mu\right)/\partial x = 0 \tag{5}$$

with such initial conditions valid if $t = 0$ and $x \in \overline{I}$

$$p = \rho g(L - x) + \mu_1 m V_0 x\left(f_\theta(\alpha_1 x) - 1\right)/K, \tag{6}$$

$$\tilde{c} = \left(1 - f_\theta(\alpha_0 x)\right) \cdot c_{imp} \tag{7}$$

and boundary conditions

$$\partial p/\partial x = -\mu_1 m V_0 \left(1 - f_\theta(\alpha_1 x) - x\, df_\theta(\alpha_1 x)/dx\right)/K - \rho \cdot g, \tag{8}$$

$$c = c_{imp}\left(1 - f_\theta(-\alpha_0 \varepsilon)\right) \tag{9}$$

where $(x,\ t) \in A_{T,1}$ and

$$p = \mu_1 m V_0 L\left(f_\theta(\alpha_1 L) - 1\right)/K, \tag{10}$$

$$\partial c/\partial x = -c_{imp}\left(df_\theta(\alpha_0 x)/dx\right)\left(a_L V_{L,0} + D^*\right)/\left(a_L V + D^*\right) \tag{11}$$

where $(x,\ t) \in A_{T,2}$.

In this model at any moment of time t such that $0 < t < L/V_0$ the injection front position is determined by high gradient regions of cement concentration and pore fluid pressure space distributions. The positions of

these regions are changing with time and are not known in advance. Therefore, in this work we are looking for each numerical space distribution evolution in the form of the sum of two functions. The first one is modeling the evolution of the respective distribution high gradient region, while the second one does not have such region. Although condition (1) is not satisfied according to estimations made in the second section, the solution of the injection test model with a free moving boundary can provide a good start for the model function construction.

A grouting model with a free moving boundary. In this section we develop a mathematical model with a free moving boundary of the standard laboratory test described in the second section for the injection duration T such that $T < L/V_0$. We assume that the grout penetrates the water saturated sand filling the tube a distance $x_0 = V_0 t$ from the injection point by the moment of time t. We chose the upward direction as positive direction of x_3 axis and place the coordinate origin in the center of the bottom tube side. We assume that by the moment of time t the sand in the bottom part of the tube $\left(0 < x_3 < V_0 t\right)$ is saturated with cement grout, while the sand in the upper part of the tube $\left(V_0 t < x_3 < L\right)$ is saturated with water. Since the solution of this model is used for a model function construction, we assume that water and grout densities are identical and equal ρ. In this section we use the following notations. Ω is a circle (a set of points $\left(x_1,\, x_2\right)$: $\sqrt{x_1^2 + x_2^2} < R$) where R is the tube radius. $Q_1(t) = \Omega \times \left(0,\, V_0 t\right)$ is a cylinder (a set of points $\left(x_1,\, x_2,\, x_3\right)$: $\left(x_1,\, x_2\right) \in \Omega$, $x_3 \in \left(0,\, V_0 t\right)$), S_1 is the bottom base of $Q_1(t)$ (a set of points $\left(x_1,\, x_2,\, x_3\right)$: $\left(x_1,\, x_2\right) \in \Omega$, $x_3 = 0$), S_2 is the side surface of $Q_1(t)$ (a set of points $\left(x_1,\, x_2,\, x_3\right)$: $x_1^2 + x_2^2 = R^2$, $x_3 \in \left(0,\, V_0 t\right)$), $Q_2(t) = \Omega \times \left(V_0 t,\, L\right)$ is a cylinder (a set of points $\left(x_1,\, x_2,\, x_3\right)$: $\left(x_1,\, x_2\right) \in \Omega$, $x_3 \in \left(V_0 t,\, L\right)$), S_3 is the top base of $Q_1(t)$ or the bottom base of $Q_2(t)$ (a set of points $\left(x_1,\, x_2,\, x_3\right)$: $\left(x_1,\, x_2\right) \in \Omega$, $x_3 = V_0 t$), S_4 is the side surface of $Q_2(t)$ (a set of points $\left(x_1,\, x_2,\, x_3\right)$: $x_1^2 + x_2^2 = R^2$, $x_3 \in \left(V_0 t,\, L\right)$), S_5 is the top base of $Q_2(t)$ (a set of points $\left(x_1,\, x_2,\, x_3\right)$: $\left(x_1,\, x_2\right) \in \Omega$, $x_3 = L$). The ground skeleton is regarded as absolutely rigid. Therefore, at any moment of time t such that $0 < t < L/V_0$ the head function

$$h_1 = p_1\left(x_1, x_2, x_3, t\right)\big/\rho/g + x_3, \tag{12}$$

where p_1 is the grout pressure satisfies at any point $(x_1,\ x_2,\ x_3)$ such that $(x_1,\ x_2,\ x_3) \in Q_1(t)$ the following equation [7, p. 38]

$$\Delta h_1 = \partial^2 h_1 / \partial x_1^2 + \partial^2 h_1 / \partial x_2^2 + \partial^2 h_1 / \partial x_3^2 = 0 \qquad (13)$$

and satisfies on the boundary of $Q_1(t)$ the following conditions:

$$\left.\frac{\partial h_1}{\partial \vec{n}_1}\right|_{S_1} = \frac{m \cdot \mu_1 \cdot V_0}{K \cdot \rho \cdot g},\ \left.\frac{\partial h_1}{\partial \vec{n}_2}\right|_{S_2} = 0,\ \left.\frac{\partial h_1}{\partial \vec{n}_3}\right|_{S_3} = -\frac{m \cdot \mu_1 \cdot V_0}{K \cdot \rho \cdot g}. \qquad (14)$$

In equations (14) $\vec{n}_i$ is external with respect to the interior of $Q_1(t)$ and normal to S_i unit vector where $i = \overline{1,3}$. At the same moment of time t the head function

$$h_2 = p_2(x_1, x_2, x_3, t) / \rho / g + x_3 \qquad (15)$$

where p_2 is the water pressure satisfies at any point $(x_1,\ x_2,\ x_3)$ such that $(x_1,\ x_2,\ x_3) \in Q_2(t)$ the following equation [7, p. 38]

$$\Delta h_2 = \partial^2 h_2 / \partial x_1^2 + \partial^2 h_2 / \partial x_2^2 + \partial^2 h_2 / \partial x_3^2 = 0 \qquad (16)$$

and satisfies on the boundary of $Q_2(t)$ the following conditions:

$$\left.\frac{\partial h_2}{\partial \vec{l}_3}\right|_{S_3} = \frac{m \cdot \mu_2 \cdot V_0}{K \cdot \rho \cdot g},\ \left.\frac{\partial h_2}{\partial \vec{l}_4}\right|_{S_4} = 0,\ \left.\frac{\partial h_2}{\partial \vec{l}_5}\right|_{S_5} = -\frac{m \cdot \mu_2 \cdot V_0}{K \cdot \rho \cdot g},\ h\big|_{S_5} = L. \qquad (17)$$

In equations (17) $\vec{l}_i$ is external with respect to the interior of $Q_2(t)$ and normal to S_i unit vector where $i = \overline{3,5}$. In addition, we assume that at any moment of time t the pore fluid pressure is continuous on S_3

$$(h_1 - x_3)\big|_{S_3} = (h_2 - x_3)\big|_{S_3}. \qquad (18)$$

Definition 1. The classical solution of the system of the boundary problems (13), (14), (16)–(18) is a pair of functions $h_1(x_1, x_2, x_3, t)$ and $h_2(x_1, x_2, x_3, t)$ with the following properties.

1. If $(x_1,\ x_2,\ x_3) \in Q_1(t)$ $\left((x_1,\ x_2,\ x_3) \in Q_2(t)\right)$, then all derivatives of function $h_1(x_1, x_2, x_3, t)$ $\left(h_2(x_1, x_2, x_3, t)\right)$ with respect to variables x_1, x_2, and x_3 up to the second order at any fixed t such that $0 < t < L/V_0$ are continues.

2. If $(x_1, x_2, x_3) \in \bar{Q}_1(t)$ $\left((x_1, x_2, x_3) \in \bar{Q}_2(t)\right)$, then function $h_1(x_1, x_2, x_3, t)$ $\left(h_2(x_1, x_2, x_3, t)\right)$ and all its first derivatives with respect to variables x_1, x_2, and x_3 at any fixed t such that $0 < t < L/V_0$ are continues.
3. If $(x_1, x_2, x_3) \in Q_1(t)$ $\left((x_1, x_2, x_3) \in Q_2(t)\right)$, then function $h_1(x_1, x_2, x_3, t)$ $\left(h_2(x_1, x_2, x_3, t)\right)$ satisfies equation (13) ((16)) at any fixed t such that $0 < t < L/V_0$.
4. At any fixed t such that $0 < t < L/V_0$ function $h_1(x_1, x_2, x_3, t)$ satisfies the first equation, the second one, and the third one of equations (14) on S_1, S_2, and S_3 respectively.
5. At any fixed t such that $0 < t < L/V_0$ function $h_2(x_1, x_2, x_3, t)$ satisfies the first equation and the second one of equations (17) on S_3 and S_4 respectively.
6. At any fixed t such that $0 < t < L/V_0$ function $h_2(x_1, x_2, x_3, t)$ satisfies the third equation and the fourth one of equations (17) on S_5.
7. At any fixed t such that $0 < t < L/V_0$ functions $h_i(x_1, x_2, x_3, t)$ where $i = 1, 2$ satisfy equation (18) on S_3.

Theorem 1. If the classical solution of boundary problem system (13), (14), (16)–(18) exists, then it is unique.

Proof. Let us assume that there are two classical solutions of boundary problem system (13), (14), (16)—(18) $h_i(x_1, x_2, x_3, t)$ and $\tilde{h}_i(x_1, x_2, x_3, t)$ where $i = \overline{1,2}$. To prove that $h_i(x_1, x_2, x_3, t) \equiv \tilde{h}_i(x_1, x_2, x_3, t)$ where $i = \overline{1,2}$, we denote their difference in the following way

$$w_i = h_i(x_1, x_2, x_3, t) - \tilde{h}_i(x_1, x_2, x_3, t), \ i = \overline{1,2}. \qquad (19)$$

If two functions $u(x_1, x_2, x_3)$, $v(x_1, x_2, x_3)$, and all their first derivatives are continuous on $\bar{Q}_i(t)$, and all their second derivatives are continuous on $Q_i(t)$ where $i = 1$ or $i = 2$, then the following Green's formula holds [9, p. 291]

$$\iiint\limits_{Q_i(t)} u \Delta v \, d\tau = -\iiint\limits_{Q_i(t)} \sum_{j=1}^{3} \left(\partial u / \partial x_j\right)\left(\partial v / \partial x_j\right) d\tau + \iint\limits_{\Sigma_i(t)} u \left(\partial v / \partial n\right) d\sigma. \qquad (20)$$

Here $\Sigma_i(t)$ is the piecewise-smooth boundary of $Q_i(t)$, $d\tau = dx_1 dx_2 dx_3$ is a volume element, $d\sigma$ is an area element. Substituting w_i where $i = 1$ or $i = 2$ in (20) instead of u and v, we get

$$\iiint\limits_{Q_i(t)} w_i \Delta w_i d\tau = -\iiint\limits_{Q_i(t)} \sum_{j=1}^{3} \left(\partial w_i / \partial x_j\right)^2 d\tau + \iint\limits_{\Sigma_i(t)} w_i \left(\partial w_i / \partial n\right) d\sigma . \quad (21)$$

Since $\Delta h_1 = \Delta \tilde{h}_1 = 0$ in $Q_1(t)$ and $\Delta h_2 = \Delta \tilde{h}_2 = 0$ in $Q_2(t)$, the left hand side of equation (21) equals zero. Since the normal derivative of w_1 is equal to zero on surface S_i where $i = \overline{1,3}$, and the normal derivative of w_2 is equal to zero on surface S_j where $j = \overline{3,5}$, the surface integral in the right hand side of equation (21) is equal to zero. Therefore, from equation (21) it follows that

$$\iiint\limits_{Q_i(t)} \left(\left(\partial w_i / \partial x_1\right)^2 + \left(\partial w_i / \partial x_2\right)^2 + \left(\partial w_i / \partial x_3\right)^2 \right) d\tau = 0 .$$

An integral of a sum of squares can be equal to zero only if each of additives is equal to zero:

$$\partial w_i / \partial x_1 = 0 , \ \partial w_i / \partial x_2 = 0 , \ \partial w_i / \partial x_3 = 0 . \quad (22)$$

(22) implies that $w_i = c_i$ in $Q_i(t)$ where c_i is a constant and $i = 1, 2$. Since $w_2 = 0$ on S_5, c_2 is equal to zero. From equations (18) and (19) it follows that on S_3 the following equality holds $c_1 = c_2$. Therefore, c_1 equals zero. Thus, we proved that $w_i \equiv 0$ where $i = 1, 2$. The theorem is proved.

Theorem 2. If $0 < t < L/V_0$, then the pair of functions

$$h_1(x_1, x_2, x_3, t) = \frac{mV_0\mu_1}{K\rho g}\left(V_0 t - x_3\right) + \left(1 + \frac{mV_0\mu_2}{K\rho g}\right)\left(L - V_0 t\right) + V_0 t , \quad (23)$$

$$h_2(x_1, x_2, x_3, t) = \left(L - x_3\right) mV_0\mu_2 / K / \rho / g + L \quad (24)$$

is the classical solution of boundary problem system (13), (14), (16)—(18). In (23) and (24) $(x_1, x_2, x_3) \in \overline{Q}_1$ and $(x_1, x_2, x_3) \in \overline{Q}_2$ respectively.

Proof. From equations (23) and (24) it follows that functions $h_1(x_1, x_2, x_3, t)$ and $h_2(x_1, x_2, x_3, t)$ satisfy the first two properties from definition 1. Substituting the right hand side of equation (23) in equations (13), (14), and (18) instead of $h_1(x_1, x_2, x_3, t)$ and the right hand side of equation (24) in equations (16)–(18) instead of $h_2(x_1, x_2, x_3, t)$, it is easy to check that functions $h_1(x_1, x_2, x_3, t)$ and $h_2(x_1, x_2, x_3, t)$ satisfy properties 3—7 from definition 1. Thus, the pair of functions $h_1(x_1, x_2, x_3, t)$ and $h_2(x_1, x_2, x_3, t)$ is the classical solution of boundary problem system (13), (14), (16)—(18). The theorem is proved.

From equations (12) and (23) it follows that if $0 < t < L/V_0$ and $(x_1, x_2, x_3) \in \bar{Q}_1(t)$, then

$$p_1 = (L - V_0 t)(\rho g + \mu_2 m V_0 / K) - (\rho g + \mu_1 m V_0 / K)(x_3 - V_0 t). \quad (25)$$

In its turn, from equations (15) and (24) it follows that if $0 < t < L/V_0$ and $(x_1, x_2, x_3) \in \bar{Q}_2(t)$, then

$$p_2 = (\mu_2 m V_0 / K + \rho g)(L - x_3). \quad (26)$$

In this model it is assumed that at any moment of time t such that $0 < t < L/V_0$ the cement concentration is equal to c_{imp} in $Q_1(t)$ and equals zero in $Q_2(t)$. Therefore, assuming $x = x_3$ the solution of this model can be written in the form

$$p(x,t) = p_1(x,t) + \theta(x - V_0 t)(p_2(x,t) - p_1(x,t)), \quad (27)$$

$$c(x,t) = (1 - \theta(x - V_0 t)) \cdot c_{imp} \quad (28)$$

where $\theta(x - V_0 t)$ is calculated according to equation (3) and $p_1(x,t)$, $p_2(x,t)$ are calculated according to equations (25) and (26) respectively.

Model function construction. During an injection a transition zone separates the domain in which the cement concentration is equal to c_{imp} from the zero concentration one. The concentration is monotonic continuous function inside this transition zone. If condition (1) is satisfied, then this zone is narrow with respect to the first domain [3, p. 61–63]. In this case, assuming that the sand column is sufficiently high, this zone can be treated as a sharp boundary between fluid in which the concentration equals c_{imp} and zero concentration one. As it was shown in the second section, condition (1) is not satisfied in the modeled test. This condition is derived, analyzing the analytical solution of the following partial differential equation valid for $0 < x < +\infty$ and $t > 0$

$$\tilde{D}\,\partial^2 c / \partial x^2 - \tilde{V}\,\partial c / \partial x = \partial c / \partial t \quad (29)$$

where $\tilde{D}$ and $\tilde{V}$ are positive constants with the following initial and boundary conditions valid for $0 < x < +\infty$ and $t > 0$:

$$c(x,0) = 0,\ c(\infty,t) = 0,\ c(0,t) = c_0 \quad (30)$$

where c_0 is a positive constant. Equations (29), (30) do not contain the acceleration of free fall. Comparing equation (29) and equation (4) one can assume (assumption #1) that the gravity force causes the shift of the injection front velocity ΔV equal to $-K\rho g / \mu$. Therefore, to construct the

function modeling the pore fluid pressure high gradient region evolution, we need to substitute $f_\theta\left(\alpha_p\left(x-V_1t\right)\right)$ instead of $\theta\left(x-V_0t\right)$ in equation (27) where here and bellow $V_1=V_0-K\rho g/\mu_{eff}$, α_p is a large constant, μ_{eff} is defined below. In addition, we need to substitute

$$\tilde{p}_1=\left(L-V_1t\right)\left(\rho g+\mu_2 mV_1/K\right)-\left(\rho g+\mu_1 mV_{eff}/K\right)\left(x-V_1t\right), \quad (31)$$

where V_{eff} is defined below and

$$\tilde{p}_2=\left(\mu_w mV_1/K+\rho g\right)\left(L-x\right) \quad (32)$$

instead of $p_1\left(x,t\right)$ and $p_2\left(x,t\right)$ respectively in equation (27). In its turn, to construct the function modeling the cement concentration high gradient region evolution, we need to substitute $f_\theta\left(\alpha_c\left(x-V_1t\right)\right)$ where α_c is a large constant instead of $\theta\left(x-V_0t\right)$ in equation (28). To estimate the model calculation error properly we need to use two methods to find the numerical solution of problem (4)—(11). In the first one the problem (4)—(11) is discretized at once, while in the second one we are looking for the numerical solution in the form

$$p\left(x,t\right)=p^{(0)}\left(x,t\right)+p^{(1)}\left(x,t\right),\ c\left(x,t\right)=c^{(0)}\left(x,t\right)+c^{(1)}\left(x,t\right),$$

where

$$p^{(0)}\left(x,t\right)=\tilde{p}_1\left(x,t\right)+f_\theta\left(\alpha_p\left(x-V_1t\right)\right)\left(\tilde{p}_2\left(x,t\right)-\tilde{p}_1\left(x,t\right)\right), \quad (33)$$

$$c^{(0)}\left(x,t\right)=\left[1-f_\theta\left(\alpha_c\left(x-V_1t\right)\right)\right]\cdot c_{imp}. \quad (34)$$

Performing calculations by the second method we assume (assumption №2) that calculation results obtained when $\mu_{eff}=\left(\mu_1+\mu_2\right)/2$ and $V_{eff}=\left(V_0+V_1\right)/2$ do not sufficiently deviate from ones obtained when $\mu_{eff}=\sqrt{\mu_1\cdot\mu_2}$ and $V_{eff}=\sqrt{V_0\cdot V_1}$. Functions $p^{(0)}\left(x,t\right)$ and $c^{(0)}\left(x,t\right)$ are modeling high gradient region evolutions of pore fluid pressure and cement concentration respectively. In equation (33) $\tilde{p}_1\left(x,t\right)$ and $\tilde{p}_2\left(x,t\right)$ are calculated according to equations (31) and (32) respectively.

Analyzing the analytical solution of problem (29), (30) it was shown in [3, p. 62] that the transition zone width is equal to $2\cdot\sqrt{8Dt}$. Using data from Table 1 and estimation (2) one can estimate $D_h\approx a_LV$. Since $Vt_1<8a_L$, $Vt_2>8a_L$, $Vt_3>8a_L$ where $t_1=100\ s$, $t_2=250\ s$, $t_3=400\ s$ and, taking into account that problem (29), (30) is a rough model of the injection test at hand, we assume that the half of the transition zone width, which we denote

δ, is given by the following expression $\delta = 8a_L$. We define the half of the transition zone width as the solution of the following equation

$$1 - f_\theta\left(\alpha_c \delta\right) = 1/e^r \tag{35}$$

where r is such that $r > \ln(2)$, and a method of its numerical determination is described at the end of this section. Performing calculations by the second method we assume that if the order of magnitude of the value of α_p in the right hand side of equation (33) is the same as the order of magnitude of the value of α_c in the right hand side of equation (34), then numerical solution is not sensitive to the choice of the value of α_p (assumption №3). Therefore, in what follows we assume that $\alpha_p = \alpha_c$. Assuming $\delta = 8a_L$ we find the value of α_c solving equation (35).

To find the numerical solution of problem (4)—(11) we cover $\overline{I}_T$ with uniform grid $\Omega_{N,M} = \left(\left(x_i,\, t_j\right),\, x_i = -\varepsilon + i \cdot h,\; i = \overline{0,N};\;\; t_j = j \cdot \tau,\, j = \overline{0,M}\right)$ where $h = \left(L + \varepsilon\right)/N$ and $\tau = T/M$.

Performing an analysis of numerical solutions of problem (4)—(11) one can use the following measure of a difference between two space distributions of the cement concentration or the pore fluid pressure $f_1\left(x,t\right)$ and $f_2\left(x,t\right)$ at a chosen moment of time t

$$\varepsilon\left(t\right) = \max_{x \in [0,\, L]} \left| f_1\left(x,t\right) - f_2\left(x,t\right) \right|.$$

We denote the measure of the difference between the space distribution of the cement concentration (the pore fluid pressure) at a given moment of time obtained by the second method on grid $\Omega_{2N_1,2N_2}$ and the one obtained by the second method on grid Ω_{N_1,N_2} as ε_1^c $\left(\varepsilon_1^p\right)$. We denote the measure of the difference between the space distribution of the cement concentration (the pore fluid pressure) at a given moment of time obtained by the first method on grid $\Omega_{2N_1,2N_2}$ and the one obtained by the second method on the same grid $\Omega_{2N_1,2N_2}$ as ε_2^c $\left(\varepsilon_2^p\right)$. An approximation error of the discretized problem depends not only on the grid increment, but also on high order derivatives of the sought for function. For instance, substituting the central difference formula instead of a function partial derivative in a nodal point $\left(x_i,t_j\right)$ of $\Omega_{N,M}$ and assuming that h is sufficiently small, the following approximate equality holds

$$\frac{\partial f\left(x_i,t_j\right)}{\partial x}-\frac{\left(f\left(x_i+h,t_j\right)-f\left(x_i-h,t_j\right)\right)}{2h}\approx\frac{h^2}{6}\cdot\frac{\partial^3 f\left(x_i,t_j\right)}{\partial x^3},$$

where

$$\frac{\partial f\left(x_i,t_j\right)}{\partial x}=\left.\frac{\partial f\left(x,t_j\right)}{\partial x}\right|_{x=x_i},\quad \frac{\partial^3 f\left(x_i,t_j\right)}{\partial x^3}=\left.\frac{\partial^3 f\left(x,t_j\right)}{\partial x^3}\right|_{x=x_i}.$$

If the sought function contains high gradient region, then its high order derivatives are large in this region. Ideally, if the value of r is chosen correctly, then functions $c^{(1)}\left(x,t\right)$ and $p^{(1)}\left(x,t\right)$ do not contain such regions. Therefore, ε_1^c and ε_1^p are minimal at such value of r.

It follows from equations (27), (28) that across the high gradient region the value of the cement concentration in the fluid phase varies from c_{imp} to zero and the value of the derivative of the fluid pore pressure with respect to space coordinate varies approximately from $-\rho g-\mu_1 mV_0/K$ to $-\rho g-\mu_2 mV_0/K$.

The high gradient region of the numerical solution obtained by the first method on a uniform grid is dispersed. We give it the following explanation. If a nodal point $x=x_i$, $t=t_j$ where $0<i<N$ and $0<j<M$ belongs to the high gradient region, then the calculation of the first derivative of the cement concentration with respect to the space coordinate and the calculation of the second derivative of the pore fluid pressure with respect to the space coordinate at this point according to the following formulas

$$\partial c\left(x,t_j\right)\Big/\partial x=\left(c\left(x_i+h,t_j\right)-c\left(x_i-h,t_j\right)\right)\Big/2/h,$$

$$\partial^2 p\left(x,t_j\right)\Big/\partial x^2=\left(p\left(x_i-h,t_j\right)-2\cdot p\left(x_i,t_j\right)+p\left(x_i+h,t_j\right)\right)\Big/h^2$$

give values smaller than respective real ones. Therefore, according to Taylor expansion the numerical cement concentration function and the numerical first derivative of the pore fluid pressure with respect to the space coordinate reach their limiting values at a distance from the nodal point larger than real one. If the value of r used in calculations is close to real one, then the high gradient region of the numerical solution obtained by the second method on a uniform grid is sharp. Therefore, in numerical experiments we need to use the value of r at which the ratios $\varepsilon_2^c/\varepsilon_1^c$ and $\varepsilon_2^p/\varepsilon_1^p$ are maximal.

Conclusions. The method of the proper treatment of high gradient regions in sought functions during numerical calculations according to model [5, p. 48—50] is developed.

Afterwards, the analysis of numerical solutions of model [5, p. 48—50] will be performed. The values of constants α_0, α_1, α_c, α_p, ε, and r will be chosen, the calculation error will be estimated, and assumptions № 1—3 will be checked as a result of this analysis. The calculations according to the models with free moving boundaries will be performed on relatively dense grids. The investigation will be conducted to check the hypothesis that in a model of the real scale cement grout injection in sand (condition (1) is satisfied) the deep bed filtration can be neglected.

References

1. Веригин Н. Н. Нагнетание вяжущих растворов в горные породы в целях повышения прочности и водонепроницаемости оснований гидротехнических сооружений / Н. Н. Веригин // Изв. Акад. Наук СССР, отд. техн. наук, 1952. — № 5. — С. 674–687.
2. Власюк А. П. Застосування числових конформних відображень до розв'язання крайової задачі з рухомою межею для рівняння параболічного типу у криволінійному чотирикутнику / А. П. Власюк, М. Б. Демчук, М. М. Обезюк // Вісн. Нац. ун-ту водн. госп-ва та природокористув, 2007. — Вип. 4 (40), ч. 3. — С. 268–286.
3. Демчук М. Б. Математичне моделювання процесу нагнітання в'яжучого розчину в пористе середовище / М. Б. Демчук // Математичне та комп'ютерне моделювання. Сер. фіз.-мат. науки : зб. наук. пр. — Кам'янець-Подільський : Кам'янець-Подільський національний університет імені Івана Огієнка, 2010. — Вип. 4. — С. 61–75.
4. Демчук М. Б. Про моделі промислового циркулярного нагнітання цементного розчину в сухий ґрунт / М. Б. Демчук // Искусственный интеллект. — 2011. — № 2. — С. 122–130.
5. Демчук М. Б. Узгоджена модель нагнітання цементного розчину в насичене пористе середовище / М. Б. Демчук // Наукові записки НАУКМА. Серія: комп'ютерні науки. — 2011. — Т. 125. — С. 46–51.
6. Корн Г. Справочник по математике для научных работников и инженеров / Г. Корн, Т. Корн. — М. : Наука, 1968. — 720 с.
7. Полубаринова-Кочина П. Я. Теория движения грунтових вод / П. Я. Полубаринова-Кочина. — М. : Наука, 1977. — 664 с.
8. Рябенький В. С. Введение в вычислительную математику / В. С. Рябенький. — Физматлит, 2000. — 294 с.
9. Тихонов А. Н. Уравнения математической физики / А. Н. Тихонов, А. А. Самарский. — М. : Государственное издательство технико-теоретической литературы, 1953. — 679 с.
10. Федоренко Р. П. Введение в вычислительную физику / Р. П. Федоренко. — М. : Издательство Московского физико-технического института, 1994. — 526 с.
11. Bear J. Introduction to modeling of transport phenomena in porous media / J. Bear, Y. Bachmat. — Dordrecht : Kluwer Academic Publishers, 1990. — 553 p.
12. Bouchelaghem F. Mathematical and numerical filtration-advection-dispersion model of miscible grout propagation in saturated porous media / F. Bouchelag-

hem, L. Vulliet // International journal for numerical and analytical methods in Geomechanics, 2001. — Vol. 25, № 12. — P. 1195–1227.
13. Bouchelaghem F. Two large-scale injection experiments, and assessment of the advection–dispersion–filtration model / F. Bouchelaghem // Géotechnique, 2002. — Vol. 52, № 9. — P. 667–682.
14. Chupin O. Modeling of a semi-real injection test in sand / O. Chupin, N. Saiyouri, P.-Y. Hicher // Computers and Geotechnics. — 2009. — Vol. 36, Issue 6. — P. 1039–1048.
15. Chupin O. Numerical modeling of cement grout injection in saturated porous media / O. Chupin, N. Saiyouri, P.-Y. Hicher [electronic resource] : Proceedings of the 16th Engineering Mechanics conference, (University of Washington, Seatle, 2003). — The regime of an accesses to the paper.: www.ce.washington.edu/em03/proceedings/papers/627.pdf.
16. Chupin O. The effects of filtration on the injection of cement-based grouts in sand columns / O. Chupin, N. Saiyouri, P.-Y. Hicher // Transport in porous media, 2008. — Vol. 72, № 2. — P. 227–240.
17. Dano C. Characterization of Loire river sand in the small strain domain using new bender extender elements. / C. Dano, H. Hareb, P.-Y. Hicher [electronic resource] : Proceedings of the 16th Engineering Mechanics conference, (University of Washington, Seatle, 2003). — The regime of an accesses to the paper.: www.gdsinstrumrnts.com/support/pdf/dano_bender_extender.pdf.
18. Maghous S. A model for in situ grouting with account for particle filtration / S. Maghous, Z. Saada, L. Dormieux, J. Canou, J. C. Dupla // Computers and Geotechnics, 2007. — Vol. 34, Issue 3. — P. 164–174.
19. Sharma M. M. Transport of particulate suspensions in porous media: model formulation / M. M. Sharma, Y. C. Yortsos // American Institute of Chemical Engineers Journal, 1987. — Vol. 33, № 10. — P. 1636–1643.
20. Vlasyuk A. P. Numerical solution of a problem of giving waterside structure foundation strength / A. P. Vlasyuk, M. B. Demchuk // Scientific Bulletin of Chelm. Section of mathematics and computer science, 2007. — № 1. — P. 211–222.

Описаний спосіб реалізації принципу рівномірності похибки в розрахунках згідно моделі нагнітання.

Ключові слова: *похибка методу, аналіз числових розв'язків, принцип рівномірності похибки, область високих градієнтів.*

Отримано: 02.04.2012